Available online at www.sciencedirect.com
ScienceDirect
Journal of the European Ceramic Society 28 (2008) 3097–3106
www.elsevier.com/locate/jeurceramsoc

Microstructural characterization and crystallization of $(1-x)TeO_2$–$xCdF_2$ ($x = 0.10, 0.15, 0.25$ mol) glasses

D. Tatar [a], M.L. Öveçoğlu [a], G. Özen [b,*]

[a] *Department of Metallurgical & Materials Engineering, Faculty of Chemical & Metallurgical Engineering, Istanbul Technical University, Maslak 34469, Istanbul, Turkey*
[b] *Department of Physics, Faculty of Science & Letters, Istanbul Technical University, Maslak 34469, Istanbul, Turkey*

Received 6 March 2008; received in revised form 16 May 2008; accepted 19 May 2008
Available online 21 July 2008

Abstract

The differential thermal analysis (DTA), X-ray diffractometer and scanning electron microscopy/energy dispersive spectrometer (SEM/EDS) techniques were used to investigate the microstructural characterization and the thermal behavior of the three $(1-x)TeO_2$–$xCdF_2$ ($x = 0.10, 0.15, 0.25$ mol) glasses. The effect of the heating rate, annealing temperature and CdF_2 content on the thermal and the microstructural properties of TeO_2–CdF_2 binary glasses were enquired. DTA analysis has shown that as the CdF_2 content in the glass composition increases, the value of the glass transition and the peak crystallization temperatures shift to higher values. SEM/EDS investigations have shown that the crystal formation of α-TeO_2, γ-TeO_2 and $CdTe_2O_5$ crystal phases were observed when the $0.90TeO_2$–$0.10CdF_2$ and the $0.85TeO_2$–$0.15CdF_2$ glass samples were annealed to temperatures above the crystallization temperatures. X-ray diffraction (XRD) results illustrated clearly the transformation of the metastable γ-TeO_2 phase to stable α-TeO_2 crystalline phase as the annealing temperature was increased from 385 to 425 °C for the $0.75TeO_2$–$0.25CdF_2$ glass.

Keywords: Tellurite glass; Crystallization; Microstructure

1. Introduction

Solid-state lasers are being used in various medical and military applications. The active medium of a solid-state laser comprises of a glass or crystalline host material doped with a rare-earth ion such as erbium, neodymium, thulium or transmission ions such as Cr^{3+}. The excited states of rare-earth ions are not strongly coupled with thermal vibrations of the crystalline lattice and as a result the laser threshold can be attained at relatively low pump intensities.[1–3]

The glasses when doped with rare-earth ions have great advantages over crystals since they can be easily prepared in a large variety of chemical compositions with high optical quality.[1] Among many oxide glasses, tellurite glasses are preferred over silicate and phosphate glasses due to their relatively low phonon energy, high refractive index, high dielectric constant, good corrosion resistance, thermal and chemical stability.[1,4,5] Tellurium oxide, however does not transform to the glassy state as a pure oxide under normal processing conditions. The alkali oxide or a fluoride addition to tellurium increases the glass-forming tendency by producing non-bridging oxygen sites which decrease the average coordination number of tellurium. Hence the glass formation requires modest cooling rated to prevent crystallization.[1,6]

El-Mallawany[1] suggested that the structure of the most stable crystalline phase of tellurium dioxide is tetragonal and also known as paratellurite (α-TeO_2). The α-TeO_2 has different modifications that are known as β-TeO_2, γ-TeO_2 and δ-TeO_2.[7,8] In order to differentiate these modifications from each other, arrangements of corner sharing TeO_4 units and their bonds can be investigated.[2] The earlier studies about the tellurite glasses showed that α-TeO_2 phase was not always formed.[1] For example Akagi et al. did not observe the α-TeO_2 phase in the $K_2O{\cdot}TeO_2$ binary glass system.[9] The γ-TeO_2 phase has an orthorhombic structure and is a metastable polymorph of the α-TeO_2.[5,10] It has a short-range atomic arrangement unlike the α-TeO_2 and the β-TeO_2 phases. The formation of the γ-TeO_2 phase in the glassy matrix is observed when the tellurite glass was modi-

* Corresponding author. Tel.: +90 212 285 3206; fax: +90 212 285 6386.
E-mail address: gozenl@itu.edu.tr (G. Özen).

0955-2219/$ – see front matter © 2008 Elsevier Ltd. All rights reserved.
doi:10.1016/j.jeurceramsoc.2008.05.029

fied by WO_3, Nb_2O_5 or PbO annealed at about 440 °C.[11,12] The transformation of the γ-TeO_2 phase to the stable α-TeO_2 takes place at higher temperatures. The δ-TeO_2 is described as the superposition of the α-TeO_2, β-TeO_2 and the γ-TeO_2 phases and acts as an intermediate phase in between the crystalline and the glassy structure.

An understanding of the crystallization behavior is important to develop and use TeO_2-based glasses as a laser material or an optical switching device, which will bear high thermal loads and thus crystallization is likely to occur during lasing. The relation between the crystallization and the local structure of the glasses has already been discussed in the literature for various compositions.[10,13] This study inquires about the thermal and the microstructural properties of CdF_2 containing tellurite glasses. The effect of the heating rate, annealing temperature and CdF_2 content on the thermal and the microstructural properties of TeO_2–CdF_2 binary glasses were investigated in detail.

2. Experimental procedure

2.1. Glass synthesis

Three different compositions of glasses with 0.10, 0.15 and 0.25 mol of CdF_2 content were prepared by using high purity TeO_2 (99.99% purity, Aldrich) and CdF_2 (99% purity, Aldrich) powders. Powder batches of 7 g were weighed in a Precisa™ XB220A sensitive balance and ground in an agate mortar for 5 min in order to obtain a homogenized structure. A platinum crucible with a closed lid was used for the melting processes in an electrically heated furnace at 900 °C for about 15–90 min. The molten glass was removed from the furnace at 900 °C and was cast by dipping the platinum crucible in a icy water bath for quenching.

2.2. Thermal behavior and crystallization

Differential thermal analysis (DTA) scans of as-cast $0.90TeO_2 + 0.10CdF_2$, $0.85TeO_2 + 0.15CdF_2$ and $0.75TeO_2 + 0.25CdF_2$ glass specimens were carried out in a TA™ Q600 DTA/TGA/DSC. The DTA scans were recorded using 3–15 mg as-cast glass specimens which were powdered and heated with the heating rates of 5, 10 and 20 °C/min between 20 and 1000 °C temperatures in a platinum crucible and using the same amount of alumina powder as the reference material. TA Instruments Universal Analysis Program™ was used to determine the glass transition temperatures T_g, selected as the inflection point of the step change of the calorimetric signal and the T_p temperatures measured at the peak of crystallization. The effects of different heating rates on the crystallization peak temperatures (T_p) were also examined through the DTA curves recorded with the heating rates of 5, 10 and 20 °C/min. The heat-treated glass samples were prepared by heating the as-cast glasses above the crystallization peak temperatures obtained from the DTA analyses and quenched immediately by immersing the platinum crucible into water.

2.3. Microstructural characterization

Optical microscopy (OM) was performed with a Nikon™ Eclipse L150 microscope equipped with Nikon™ Coolpix 4.0 MP digital camera. Scanning electron microscopy (SEM) was carried out both in a JEOL™ Model JSM 5410 operated at 15 kV and linked with Noran™ 2100 Freedom energy dispersive spectrometer (EDS) attachment and in a JEOL™ Model JSM-T330 operated at 25 kV and linked with a Zmax 30 Boron-up light element EDS detector. For the OM and SEM investigations, optical mount specimens were prepared using standard metallographic techniques followed by chemical etching in a 95% distilled water +5% HF solution for 10–20 s. The etched optical samples were coated with palladium–gold for the SEM and SEM/EDS observations. X-ray diffraction (XRD) technique of the glasses scanned with the heating rates of 5, 10 and 20 °C/min glasses to certain annealing temperatures was performed using a Bruker™ D8 Advanced Series powder diffractometer and was used for acquiring the glass structure and the identification of the crystallized phases. All traces were recorded using Cu Kα or Co Kα radiation and the diffractometer setting in the 2θ range from 10° to 90° by changing the 2θ with a step size of 0.02°. All samples were ground to fine powder for investigation and Eva Software was used to label peaks and then distinguish the crystalline phases existing in the sample. After obtaining the heat-treated glasses, ICDD (The International Centre for Diffraction Data®) data files were used for identifying the crystallized phases by comparing the intensities and the peak positions.

3. Results and discussion

In the earlier studies of Silva et al. claimed that the maximum CdF_2 content in the glass-forming TeO_2–CdF_2 binary system was 0.15 in molar ratio.[14] The present study has shown that it is possible to obtain amorphous structures with higher concentrations of CdF_2 content. Preliminary experimental results of the present investigation demonstrated the effect of the heating rate, annealing temperature and CdF_2 content on the thermal and the microstructural properties of TeO_2–CdF_2 binary glasses. The thermal properties including the crystallization behavior, were investigated using differential thermal analysis. Formation and the transformation of the crystalline phases in the microstructure of the glass samples were examined through a XRD, SEM/EDS and OM analysis.

3.1. DTA investigations

Differential thermal analysis investigations were conducted on the as-cast $0.90TeO_2 + 0.10CdF_2$, $0.85TeO_2 + 0.15CdF_2$ and $0.75TeO_2 + 0.25CdF_2$ glass samples to understand the effect of CdF_2 content and the heating rate on the thermal properties. The respective DTA thermographs of the glass samples were scanned between 200 and 800 °C at 20 °C/min heating rate are given in Fig. 1. For all scans given in Fig. 1, glass transition, T_g, peak crystallization, T_p and melting temperatures, T_m, are marked on the thermographs of the respective glasses and given in Table 1.

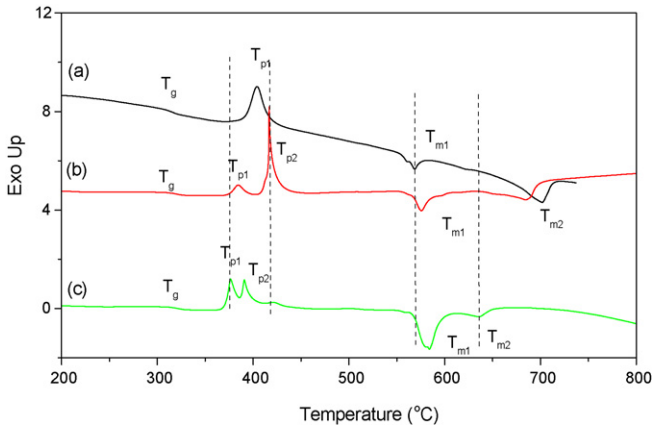

Fig. 1. DTA curves of as-cast (a) $0.90TeO_2$–$0.05CdF_2$ glass, (b) $0.85TeO_2$–$0.15CdF_2$ glass and (c) $0.75TeO_2$–$0.25\ CdF_2$ glass, scanned at a rate of 20 °C/min (vertical broken lines are drawn as a guide for the eye).

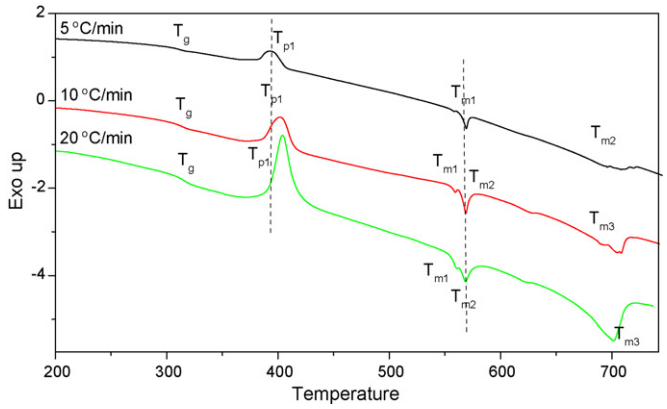

Fig. 2. DTA scans of the as-cast $0.90TeO_2$–$0.10CdF_2$ glass with different heating rates of 5, 10 and 20 °C.

It can be seen from Fig. 1 and also from Table 1 that, as the CdF_2 content in the glass composition increases, the value of the glass transition temperatures shifts to higher values in very little amounts. This behavior was also seen in other tellurite glasses having different modifiers such as Nb_2O_5.[7] On the other hand glasses containing K_2O content has shown that the T_g, shifts to lower values as the K_2O content increases.[15] As seen in Fig. 1, there are different number of peak crystallization temperatures (T_p) occurred at a range of 376–421 °C following the glass transition temperatures for three compositions. As the CdF_2 content increases from 0.10 to 0.25 in molar ratio, the number of the exothermic peaks observed on the respective thermographs also increases from one to three (Fig. 1). The maximum values of the exothermic peaks depending on the composition occur at different temperatures when the samples were scanned with the same heating rate. Hence different crystal formations occur for each exothermic peak as the CdF_2 content increases. A similar claim can also be made for the endotherms which represent the melting processes of these glasses. The first melting temperatures, T_{m1}, can be seen on very close values of the three samples so the same crystalline phase might be dissolving.

The glass-forming tendency (K_g) assessed by the difference between the first crystallization peak temperature (T_{p1}) and the glass transition temperature (T_g), is a measure of the glass thermal stability.[16,17] The thermal stability of a glass comprises the temperature interval during while the nucleation is taking place.[18] The glass stability of the certain glass system can be explain by the Hurby's parameter which is

$$K_{gl} = \frac{T_x - T_g}{T_m - T_x} \quad (1)$$

The glass-forming tendency of CdF_2 containing tellurium oxide glasses is reported to be smaller than most of the existing tellurite glasses containing different modifiers.[15,16,18–21] The K_{gl} value for each glass composition was determined from the respective DTA curve by using the lowest crystallization and the melting temperatures observed and are listed in Table 1. The thermal stability of the $0.90TeO_2$–$0.10CdF_2$ glass is 88, on the other hand this value decreases to 66 for the $0.85TeO_2$–$0.15CdF_2$ glass and 57 for the $0.75TeO_2$–$0.25CdF_2$ glass. As a result it can be said that the thermal stability of the glass decreases as the CdF_2 content in the glass increases. The value of 57 for the $0.75TeO_2$–$0.25CdF_2$ glass heated with 20 °C/min, is smaller than most of the tellurite glasses like TeO_2–LiCl which has a thermal stability value of 136 obtained with 20 °C/min heating rate, TeO_2–Nb_2O_5 which has a value 157 and TeO_2–$PbCl_2$ which has 191.[1,2,22] This consequence estimates the difficulty of obtaining CdF_2 containing glasses.

In order to investigate the effect of the heating rate on the thermal properties and the crystallization behavior of TeO_2–CdF_2 glasses DTA analysis was performed at the heating rates of 5, 10 and 20 °C/min between 200 and 800 °C and are illustrated in Figs. 2–4. These curves exhibit an endothermic transition in between 300 and 330 °C. The glass transition, crystallization peak and the melting temperature values change and shift with different heating rates for each composition.

DTA scans of the as-cast $0.90TeO_2$–$0.10CdF_2$ glass with different heating rates of 5, 10 and 20 °C are given in Fig. 2 and Table 2. Only one exothermic peak was observed in the thermographs for each heating rate. As can be seen from Fig. 2 and also Table 2, the glass transition and the crystallization temperatures of the glass composition demonstrates a very little shift to higher values with increasing scanning rates. The exothermic peak is broader when the heating rate is 5 °C/min and it becomes sharper

Table 1
Glass transition (T_g), crystallization peak and melting temperatures of the $(1-x)TeO_2$–$xCdF_2$ glasses heated with 20 °C/min rate

CdF_2 content (mol%)	T_g (°C)	T_{p1} (°C)	T_{p2} (°C)	T_{p3} (°C)	T_{m1} (°C)	T_{m2} (°C)	T_{m3} (°C)	K_g
10	316	404	–	–	569	709	–	88
15	318	384	417	–	576	684	–	66
25	319	376	391	421	583	636	676	57

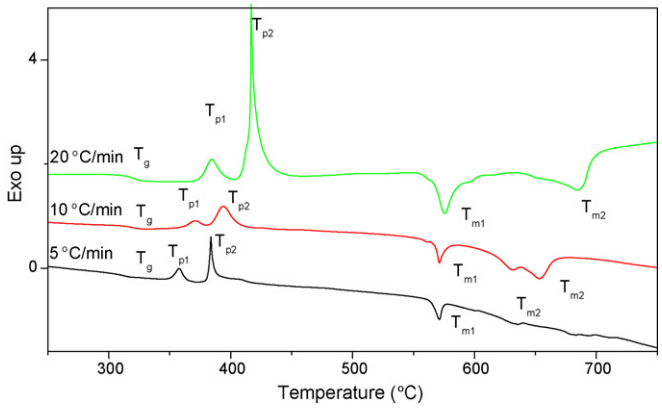

Fig. 3. DTA scans of the as-cast $0.85TeO_2$–$0.15CdF_2$ glass with different heating rates of 5, 10 and 20 °C.

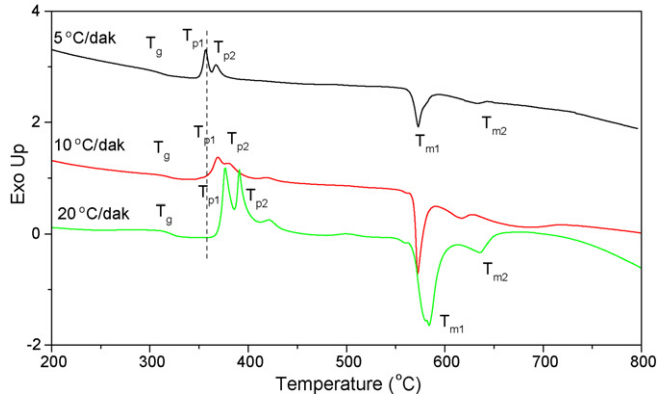

Fig. 4. DTA scans of the as-cast $0.75TeO_2$–$0.25CdF_2$ glass with different heating rates of 5, 10 and 20 °C.

Table 2
Glass transition (T_g), crystallization peak and melting temperatures of the $0.90TeO_2$–$0.10CdF_2$ glass heated with 5, 10 and 20 °C/min

Heating rate (°C/min)	T_g (°C)	T_{p1} (°C)	T_{m1} (°C)	T_{m2} (°C)	K_g
5	310	395	569	709	85
10	315	403	569	709	66
20	316	404	569	709	57

as the heating rate increases. Similar thermal behavior was also observed for the TeO_2–LiCl glasses in which the value of the glass transition and the glass crystallization peak temperatures was increased as the heating rates increased.[19,20]

DTA scans of the as-cast $0.85TeO_2$–$0.15CdF_2$ glass with different heating rates of 5, 10 and 20 °C are given in Fig. 3. As it can be seen from the figure and also Table 3, the glass transition temperature (Table 4) of the $0.85TeO_2$–$0.15CdF_2$ glass demonstrates also very little shift to higher values with increasing scanning rate. Two exothermic peaks exist for this glass composition when heated with different heating rates and these values shift to higher temperatures with higher heating rates. As it can be seen from Fig. 3. Each exothermic peak might refer to the formation or the transformation of the different crystalline phases. Following to the exotherms, also two endotherms are demonstrated in each thermograph of these glasses. Even though the first endotherm of the glasses occurred at close temperatures, the second ones varied and showed differences with different heating rates.

DTA scans of the as-cast $0.75TeO_2$–$0.25CdF_2$ glass with different heating rates of 5, 10 and 20 °C are given in Fig. 4. As it can be seen from Fig. 4 and Table 3, the glass transition temperature for this composition demonstrates also very little shift to higher values with increasing heating rate. Even though two different exotherms exist for the glasses heated with 5 and 10 °C/min, there are four exotherms for the glasses heated with 20 °C/min. It can be claimed from the temperatures of the exotherms that the first two crystallization peaks of the glasses heated with different heating rates may refer to the formation of the same phases. On the other hand the third and the fourth crystallization peaks observed when the glass heated with 20 °C/min may refer to the formation or transformation of different phases.

3.2. XRD results

The crystalline phases corresponding to the exothermic processes seen in the DTA scans were identified by using the results of the X-ray diffractometry investigations. The XRD patterns of as-cast glasses with various amount of CdF_2 content are given in Fig. 5. The spectra exhibit a broad band ranging between 26° and 42° of 2θ values which is an indication of a typical amorphous clustering observed in glassy solids. Two sharp peaks were detected for the $0.75TeO_2$–$0.25CdF_2$ as-cast glass around $2\theta = 28°$ and 43° in addition to the broad band. The Bragg angle of $\theta = 26.5°$ for the Cu Kα radiation conditions ($\theta = 0.15418$ nm) corresponds unambiguously to the highest intensity peak of the α-TeO_2.

In order to find out the formation or the transformation of the crystalline phases that may exist in these binary systems, X-ray diffractometry scans were accomplished by annealing the samples above the peak crystallization temperatures determined from the respective DTA results. The $0.90TeO_2$–$0.10CdF_2$ glass was annealed at 424, 419 and 408 °C with the heating rates of 20, 10 and 5 °C/min respectively. The XRD patterns of these annealed samples are presented in Fig. 6. The ICDD card values of the paratellurite (α-TeO_2) phase which has a tetragonal space group $P4_12_12(92)$ with lattice parameters $a = 0.481$ nm

Table 3
Glass transition (T_g), crystallization peak and melting temperatures of the $0.85TeO_2$–$0.15CdF_2$ glass heated with 5, 10 and 20 °C/min

Heating rate (°C/min)	T_g (°C)	T_{p1} (°C)	T_{p2} (°C)	T_{m1} (°C)	T_{m2} (°C)	T_{m3} (°C)	K_g
5	308	358	384	571	632	711	50
10	317	371	394	571	632	653	53
20	318	384	417	576	650	684	66

Table 4
Glass transition (T_g), crystallization peak and melting temperatures of the $(1-x)TeO_2$–$xCdF_2$ glass heated with 5, 10 and 20 °C/min

Heating rate (°C/min)	T_g (°C)	T_{p1} (°C)	T_{p2} (°C)	T_{p3} (°C)	T_{p4} (°C)	T_{m1} (°C)	T_{m2} (°C)	T_{m3} (°C)	K_g
5	310	357	367	–	–	572	632	–	47
10	318	369	381	–	–	572	616	681	51
20	319	376	391	421	500	576	650	684	57

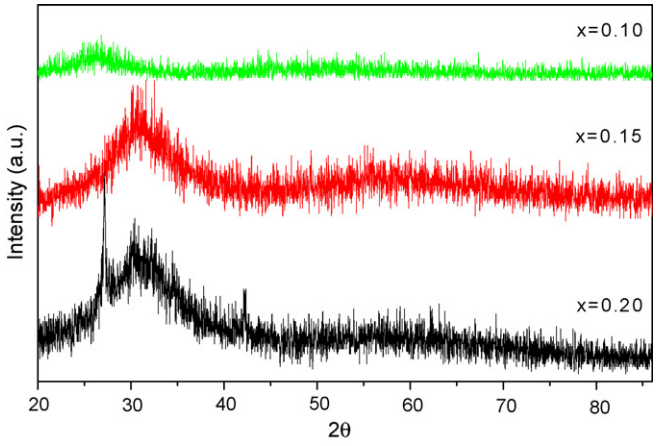

Fig. 5. X-ray diffraction patterns taken from $(1-x)TeO_2$–$xCdF_2$ glasses ($x=0.10$, 0.15, 0.25) in the as-cast condition.

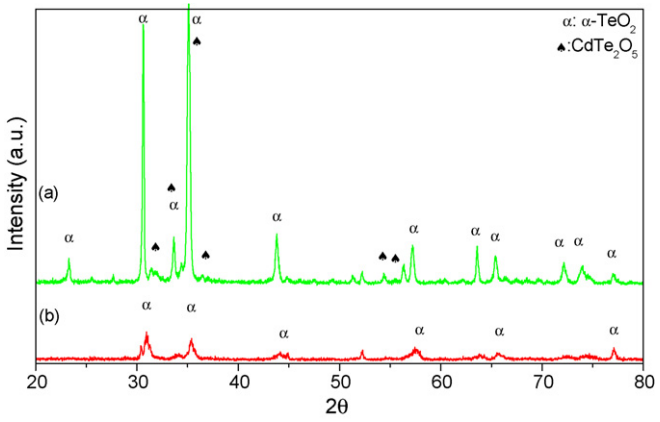

Fig. 7. X-ray diffraction patterns taken from $0.85TeO_2$–$0.15CdF_2$ glass (a) heated to 455 °C and (b) heated to 405 °C with a rate of 20 °C/min.[25,26]

and $c=0.761$ nm,[25] γ-TeO_2 phase which has a orthorhombic crystal structure and is a polymorph of paratellurite with lattice parameters $a=8.448$ nm, $b=4.993$ nm and $c=4.2995$ nm[24] and cadmium tellurium oxide ($CdTe_2O_5$) which has space group of $P2/m(10)$ and has a triclinic structure with lattice parameters of $a=6.866$ nm, $b=3.801$ nm and $c=9.098$ nm.[26] The peaks observed in all the XRD scans are identified to belong to the stable α-TeO_2, metastable γ-TeO_2 and the $CdTe_2O_5$ phases. This proofs that the scanning rate does not have an effect on the formation or the transformation of the crystalline phases in this composition.

XRD patterns of the $0.85TeO_2$–$0.15CdF_2$ glasses heated to 455 and 405 °C with a rate of 20 °C/min followed by quenching in water are given in Fig. 7. It can be seen that the formation of the α-TeO_2 phase starts at the initial step of 405 °C and no other crystal formations take place at this temperature. When the glass is annealed at 455 °C, $CdTe_2O_5$ crystalline phase was identified accompanying to the α-TeO_2 crystalline phase. The metastable phase, γ-TeO_2, was not observed in the XRD scans of the samples anneal at neither temperatures. The earlier studies show that in some of the TeO_2-based binary glass systems such as TeO_2–LiCl and TeO_2–ZnO, only crystalline phase formation observed was α-TeO_2.[2,24]

The XRD patterns of the $0.75TeO_2$–$0.25CdF_2$ glass heated to 385 and 425 °C with a rate of 20 °C/min followed by quenching in water are given in Fig. 8. When the sample was heated to 385 °C, α-TeO_2, γ-TeO_2 and $CdTe_2O_5$ crystalline phases were observed. Comparing the XRD patterns given in Figs. 7b and 8b, it can be seen that the formations of the γ-TeO_2 and $CdTe_2O_5$

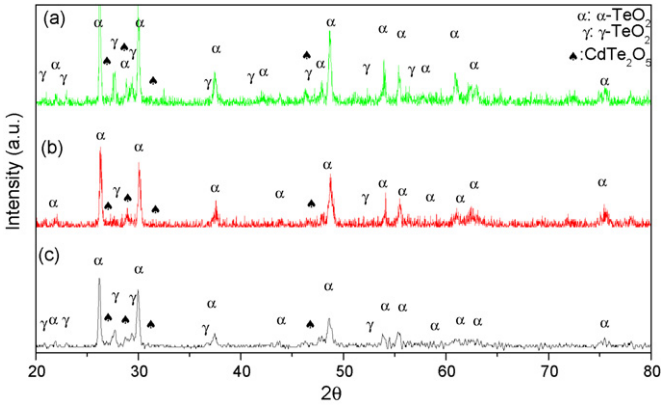

Fig. 6. X-ray diffraction patterns taken from $0.90TeO_2$–$0.10CdF_2$ glass (a) heated to 424 °C with a rate of 20 °C/min, (b) heated to 419 °C with a rate of 10 °C/min and (c) heated to 408 °C with a rate of 5 °C/min.[25,26]

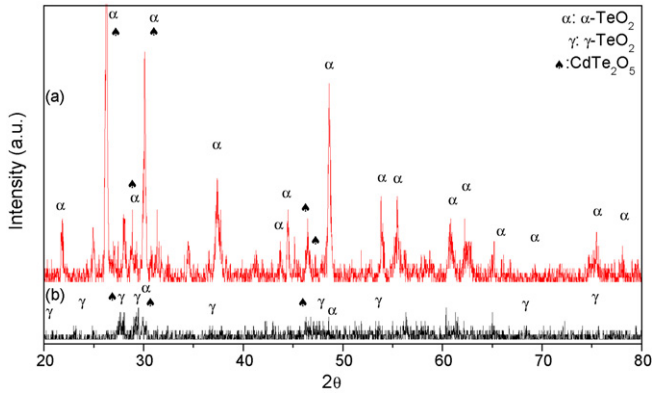

Fig. 8. X-ray diffraction patterns taken from $0.75TeO_2$–$0.25CdF_2$ glass (a) heated to 425 °C with a rate of 20 °C/min and (b) heated to 385 °C with a rate of 20 °C/min.[25,26]

phases occur when the CdF_2 content was increased from 0.15 to 0.25 mol. The transformation of the metastable γ-TeO_2 to stable α-TeO_2 can be observed clearly in the thermal behavior of this glass. When the annealing temperature increases from 385 to 425 °C as shown in Fig. 8a, the intensities of the stable α-TeO_2 also increase and the metastable γ-TeO_2 dissolves and diminishes. It can also be seen in Fig. 8 that the amount of the $CdTe_2O_5$ crystals formed in the glass also increases with the annealing temperature. The transformation of the metastable γ-TeO_2 to stable α-TeO_2 was also observed in other TeO_2-based glasses such as $0.95TeO_2$–$0.05K_2O$, $(1-x)TeO_2$ – $xZnO$ glasses at temperatures above 430 °C and also $0.85TeO_2$–$0.15WO_3$ glasses at temperatures above 440 °C.[12,15,23] On the other hand almost no structural changes were observed in TeO_2–BaO glasses heated to different annealing temperatures and the dominant γ-TeO_2 phase at lower temperatures did not disappear but lost its intensity.[16]

3.3. SEM and SEM/EDS investigations

In order to investigate the morphology of the resultant microstructures after crystallization, SEM analysis was performed on the TeO_2–CdF_2 glasses. Surface and cross-section SEM micrographs were taken in the secondary electron imaging (SEI) mode for all the samples. Fig. 9a and b are a series of surface SEM/SEI micrographs demonstrating both the surface and the cross-section of the $0.90TeO_2$–$0.10CdF_2$ glass samples heated to 408, 419 and 424 °C with different heating rates were performed and showed similar morphologies. The glasses heated to 408 and 419 °C contained disoriented needle-like crystals in smaller sizes. The crystal sizes at these annealing temperatures vary between less than 1 μm in width and about 3 and 5 μm in length. These disoriented needle-like crystals exist both in the surface and the cross-section of these glasses, hence a bulk crystallization mechanism might be taking place in this composition regardless the annealing temperature.

Fig. 9a and b are representing SEM/SEI micrographs taken from the surface and the cross-section of the $0.90TeO_2$–$0.10CdF_2$ glass heated to 424 °C with 20 °C/min. The structure reveals the presence of elongated centro-symmetric stripe-shaped crystals varying between 1 and 5 μm in width and about more than 50 μm in length. Fig. 9a and b show that there are actually two different crystal formations interconnected with each other. There are radiating crystals which are made up clover-like crystals between 20 and 60 μm in size surrounded by elongated acicular prismatic and tabular crystals also as radial nodules around them. These two different crystal formations interfere with each other and might refer to different formations of different phases. XRD scans given in Fig. 6 show the crystals that are present refer to the $CdTe_2O_5$, α-TeO_2 and/or γ-TeO_2 crystalline phases. EDS spectra taken from the acicular grains have revealed that these grains contained 27.435 wt.% Te, 1.497 wt.% Cd and 71.068 wt.% O, which indicates that they belong to a TeO_2 containing crystalline phase. Fig. 9b is a SEM/SEI representative micrograph taken from the cross-section of the $0.90TeO_2$–$0.10CdF_2$ glass sample revealing similar grains varying between 1 and 5 μm in size also exist in the cross-section parts of the glass. Thus

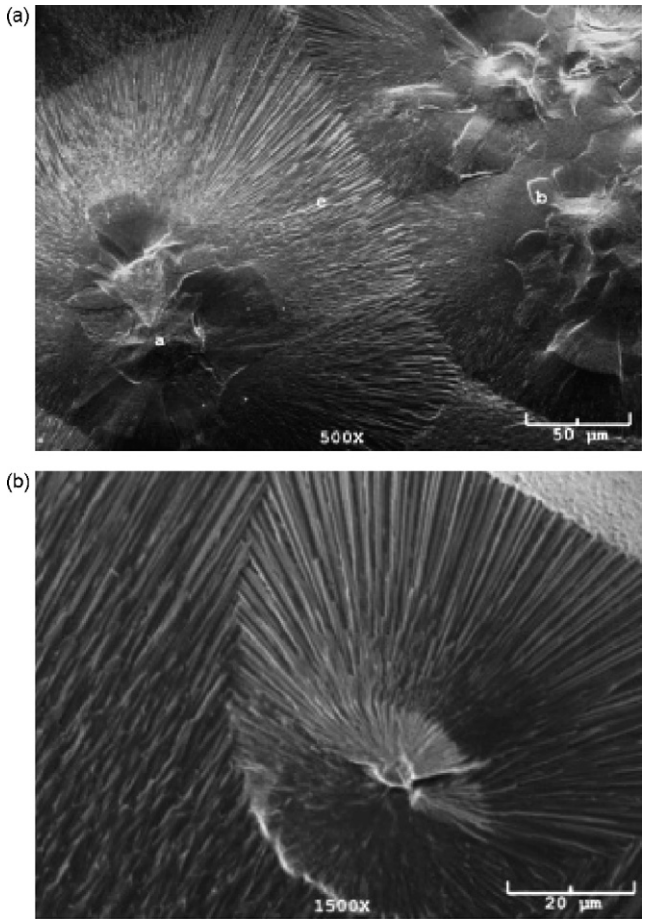

Fig. 9. Typical SEM micrographs taken from the (a) surface region, (b) cross-section of the $0.90TeO_2$–$0.10CdF_2$ glass heated to 424 °C at a rate of 20 °C/min, followed by quenching in air.

it can be inferred that bulk crystallization is the predominant mechanism for the $0.90TeO_2$–$0.10CdF_2$ glass sample. In addition, EDS spectra taken from both the clover-like crystalline grains labeled with a, contain 30.6 wt.% Te, 3.4 wt.% Cd and 66.0 wt.% O, and the regions labeled with b, contain 43.3 wt.% Te, 6.1 wt.% Cd and 50.6 wt.% O. These results confirm that the clover-like crystalline regions have higher Cd content and might reveal to the formations of a cadmium containing tellurite crystalline phase. EDS spectra taken from the needle-like crystals labeled with c, contain 27.4 wt.% Te, 1.5 wt.% Cd and 71.1 wt.% O. Considering this EDS stoichiometry, the chemistry of these regions are different than those measured from the clover-like crystalline grains. It can be concluded that the needle-like crystalline structure dominantly corresponds to the formation of the α-TeO_2 phase which has a bulk crystallization mechanism. TeO_2–LiCl glasses have trigonal-shaped paratellurite crystals between 40–50 μm in length and 7–15 μm in width for which the surface nucleation was taking place.[2] TeO_2–BaO glasses also showed α-TeO_2 formations in dendrite forms as surface crystallization.[16]

Fig. 10a and b are SEM/SEI micrographs taken from the surface and the cross-section of the $0.85TeO_2$–$0.15CdF_2$ glass heated to 405 °C with 20 °C/min. It can be seen in Fig. 10 that

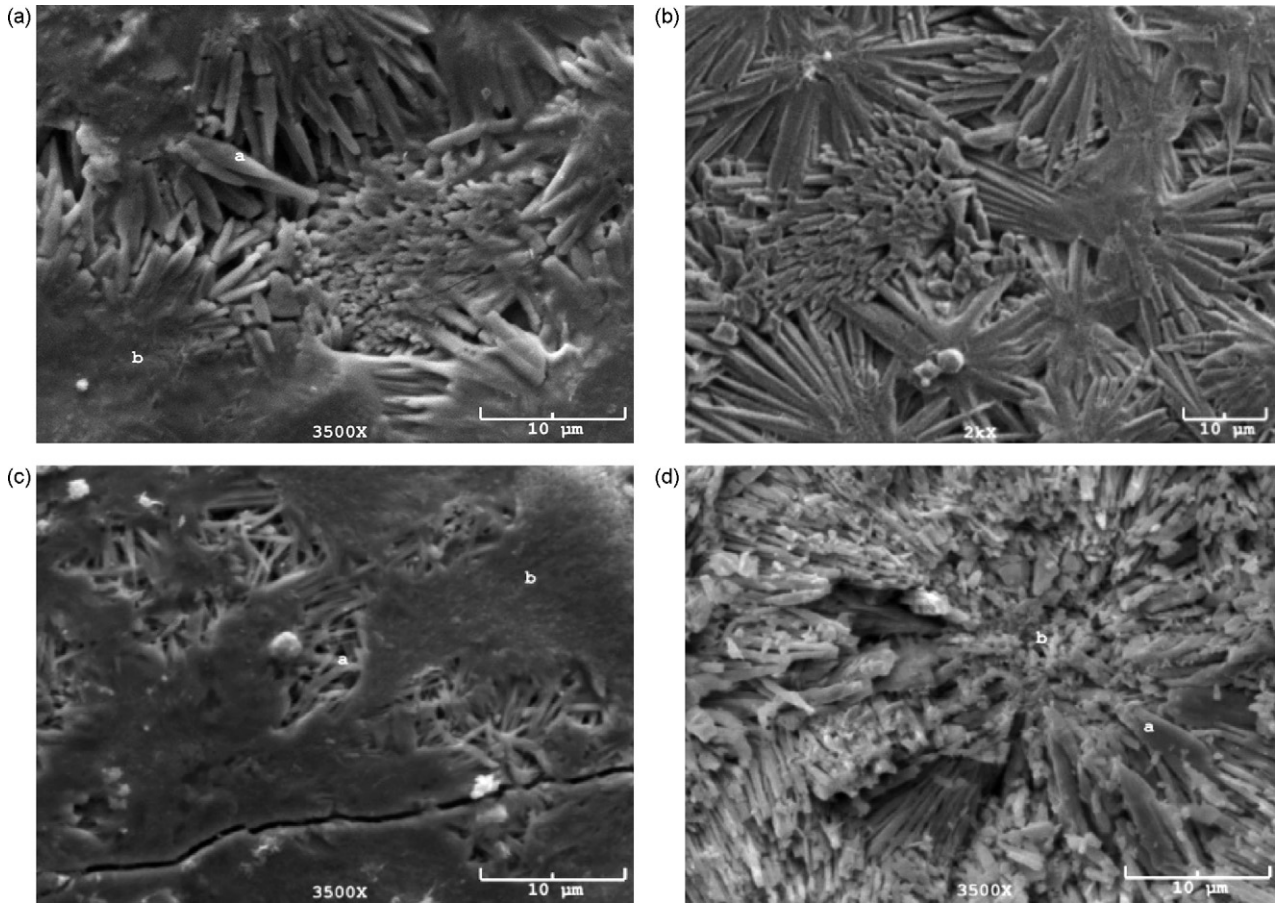

Fig. 10. Typical SEM micrographs taken from the (a) surface region, (b) cross-section of the $0.85TeO_2$–$0.15CdF_2$ glass heated to 405 °C, (c) surface region and (d) cross-section of the same sample heated to 455 °C. All samples were heated at a rate of 20 °C/min, followed by quenching in icy water.

there are radial acicular crystals in the morphology. The structure reveals the size of the crystals vary around 1 μm in width and around 10 μm in length. Images show that there is actually one type of crystal formation in agreement with the XRD scan given in Fig. 7b identified as the α-TeO_2 crystalline phase. EDS spectra taken from both the cross-section and the surface of the glass sample from the locations labeled with a contain 32.0 wt.% Te, 0.2 wt.% Cd and 67.5 wt.% O indicating that the crystals formed are α-TeO_2. On the other hand the regions labeled with b contain 26.6 wt.% Te, 1.3 wt.% Cd and 72.1 wt.% O. These results demonstrate that the parent glass matrix prevails over the α-TeO_2 crystalline phase.

SEM/SEI micrographs taken from different locations of the surface of the $0.85TeO_2$–$0.15CdF_2$ heated to 455 °C with 20 °C/min are given in Fig. 10c and d. The micrographs contain both oriented and disoriented crystallizations in the shape of needle-like acicular crystal structures. EDS spectrum, taken from the crystals labeled with a in Fig. 10c, revealed that the crystalline phase contained 19.9 wt.% Te, 13.1 wt.% Cd and 52.9 wt.% O, indicating the formation of a $CdTe_2O_5$ crystalline phase. EDS spectra taken from the crystals labeled with a and b in Fig. 10d, revealed that the crystalline phase contained 47.1 wt.% Te, 0.1 wt.% Cd and 52.9 wt.% O, indicating the formation of a TeO_2-rich crystalline phase. If the XRD scan given in Fig. 7 is reconsidered then it can be claimed that these radial acicular structures belong to the α-TeO_2 phase. Similar formations of TeO_2-rich phase was also observed in $0.85TeO_2$–$0.15WO_3$ glasses in the shape of large centro-symmetric fan-like crystals varying between 3 and 15 μm in width and about 12 and 30 μm in length.[20]

Fig. 11a and b are both surface and cross-sectional SEM micrographs taken from the $0.75TeO_2$–$0.25CdF_2$ glass sample heated to 385 °C followed by water-quenching. It is observed that similar crystal formations have taken place in this glass sample to the previous samples. Due to the XRD results of the respective glass sample given in Fig. 8, there might be the formation of γ-TeO_2 and CdT_2O_5 crystals with very little addition of α-TeO_2 in the sample. EDS spectrum, taken from the crystals labeled with c revealed that the crystalline phase contained 29.1 wt.% Te, 3.3 wt.% Cd and 67.7 wt.% O. EDS analyses show that the needle-like crystals refer to the formation of a TeO_2-rich phase in the glass body. As a consequence the crystalline phases observed in Fig. 10a and b might demonstrate the morphology of the α-TeO_2 or the γ-TeO_2 and CdT_2O_5 crystalline phases.

The microstructure of the $0.75TeO_2 + 0.25CdF_2$ glass surface and cross-section heated with 20 °C/min to 425 °C are represented in Fig. 11c and d. XRD pattern given in Fig. 8 demonstrates the transformation of the γ-TeO_2 to α-TeO_2 phase together with $CdTe_2O_5$ crystals in the glass structure. As it can be seen from the figures, the major portion of the glass matrix was

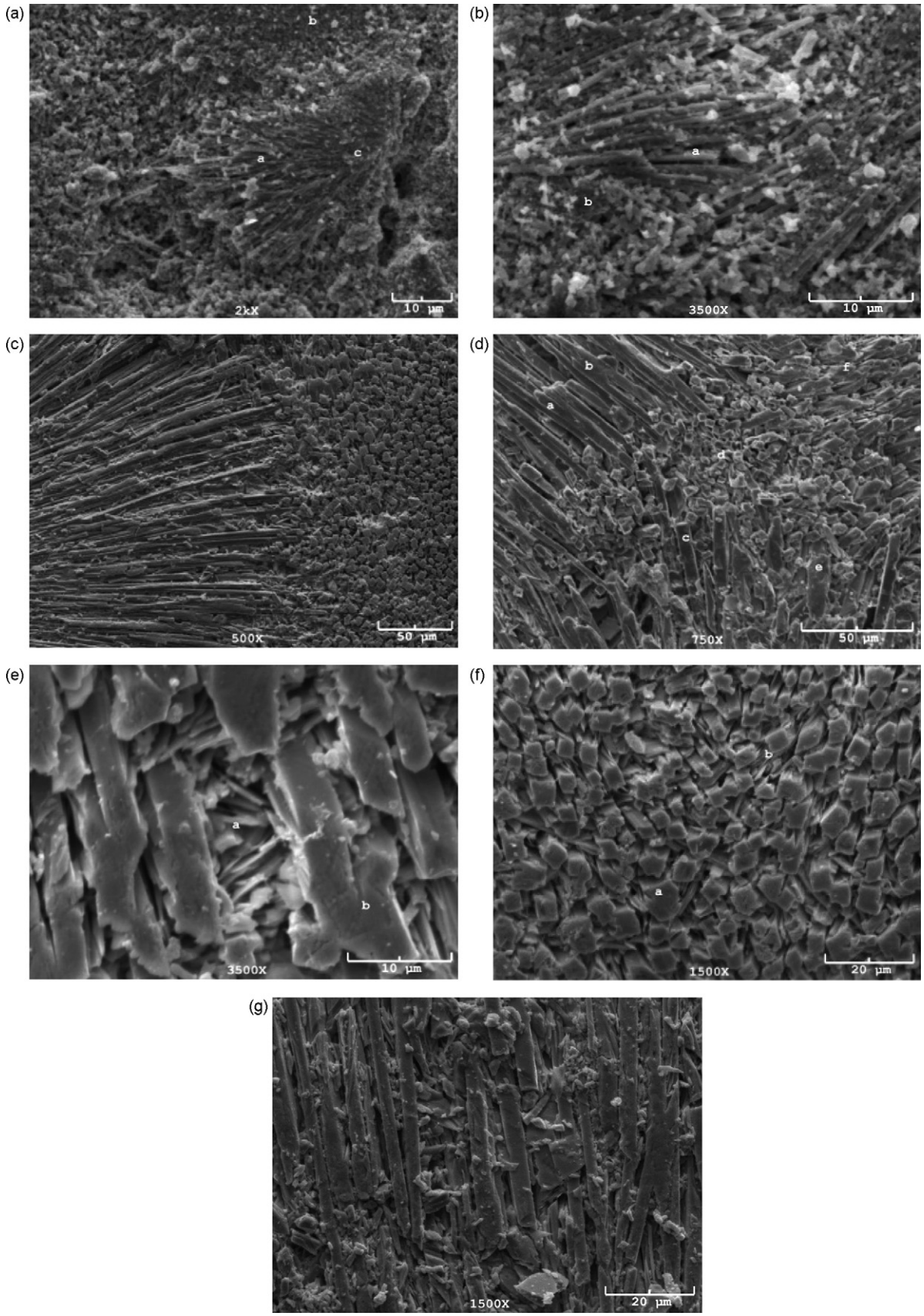

Fig. 11. Typical SEM micrographs taken from the (a) surface region, (b) cross-section of the $0.75TeO_2$–$0.25CdF_2$ glass heated to 385 °C, (c)–(f) surface region, (g) cross-section of the same sample heated to 425 °C. All samples were heated at a rate of 20 °C/min, followed by quenching in icy water.

crystallized in needle-like elongated centro-symmetric stripe-shaped crystals varying between 5 and 10 μm in width and about more than 500 μm in length. EDS spectra taken from these elongated crystalline regions in Fig. 11d revealed needle-like centro-symmetric crystals contain 80.6 wt.% Te, 0.5 wt.% Cd and 18.8 wt.% O, which confirms that these crystalline regions are TeO_2-rich regions. This result is consistent with the previous findings of the other CdF_2 containing glass structures. EDS spectra taken from Fig. 11c and d showed that there are tabular parallel to the cleavage and foliated crystals labeled with a and labeled with b which contain 26.7 wt.% Te, 9.9 wt.% Cd and 51.0 wt.% O. This confirms that these flaky crystalline regions are $CdTe_2O_5$ crystals that are formed in the glass sample. In Fig. 11d the dendrites are clearly visible and demonstrate the crystallization of α-TeO_2 phase which exists in the cross-section of the glass. Hence it can be inferred that bulk crystallization is also the predominant mechanism for the $0.75TeO_2$–$0.25CdF_2$ glass sample. It is understood that there is the existence of the $CdTe_2O_5$ crystal formation taking place in between the needle-like α-TeO_2 crystals. Similar needle-like square-shaped crystals were also observed in TeO_2–K_2O glasses.[15]

4. Conclusions

The structural role of CdF_2 modifier for the tellurium oxide glass system, and its own structural features were evidenced in the study by investigating the different compositions of CdF_2 containing glasses with varying heating rates. DTA investigations have shown that increasing the CdF_2 content in the TeO_2–CdF_2 binary glass system increases the glass transition temperature, T_g. On the other hand the increment of the modifier in the glass results in the decrement of the crystallization peaks, T_p, and the melting temperatures, T_m. The thermal stability of the glass diminishes with the increasing CdF_2 amount. The smallest value of the thermal stability determined for the $0.75TeO_2$–$0.25CdF_2$ glass evidences the difficulty of obtaining the amorphous glass structure.

Crystal formation of α-TeO_2 and $CdTe_2O_5$ crystal phases were observed when the all glass compositions were annealed above the respective crystallization temperatures. The formation of γ-TeO_2 was only observed when the $0.90TeO_2$–$0.1CdF_2$ and the $0.75TeO_2$–$0.25CdF_2$ glasses were annealed above the first crystallization peak temperatures. XRD results illustrated clearly the transformation of the metastable γ-TeO_2 phase to stable α-TeO_2 crystalline phase for the $0.75TeO_2$–$0.25CdF_2$ glass as the annealing temperature was increased from 385 to 425 °C.

SEM investigations of the surface and the cross-sections for all compositions revealed that the crystallization is three-dimensional and may refer to the bulk crystallization type. SEM and SEM/EDS investigations of the $0.90TeO_2$–$0.10CdF_2$ glass heated with different heating rates showed similar morphologies which correspond to the formations of the α-TeO_2, γ-TeO_2 and $CdTe_2O_5$ crystalline phases. The microstructures of the $0.90TeO_2$–$0.10CdF_2$, $0.85TeO_2$–$0.15CdF_2$ and $0.75TeO_2$–$0.25CdF_2$ glasses comprised elongated centro-symmetric stripe-shaped crystalline regions existed both in the surface and cross-section. SEM investigations of the $0.90TeO_2$–$0.10CdF_2$ glass showed that there are actually two different crystal formations interconnected with each other. The center of this structure was Cd-rich clover-like while the surrounding needle-like structure was Te rich. The TeO_2-rich crystalline phase has a radial needle-like morphology in all compositions where as the $CdTe_2O_5$ crystalline phase has a tabular parallel to the cleavage and foliated morphology detected in only $0.75TeO_2$–$0.25CdF_2$ glass composition.

Acknowledgements

The authors of this study express their gratitude to Çiğdem Çakır Konak for her assistance during the SEM/EDS investigations. This research has been supported by the Scientific and Research Council of Turkey (TÜBİTAK) for the financial support under the project numbered 106T347.

References

1. El-Mallawany, A. H., *Tellurite Glasses Handbook*. CRS Press, London, 2002.
2. Öveçoğlu, M. L., Özen, G., Demirata, B. and Genç, A., Microstructural characterization and crystallization kinetics of $(1-x)TeO_2$–$xLiCl$ ($x = 0.6$–0.4 mol) glasses. . *J. Eur. Ceram. Soc.*, 2007, **27**, 1823–1827.
3. Öveçoğlu, M. L., Kabalcı, İ., Özen, G. and Öz, B., Microstructural characterization of $(1-x)TeO_2$–$xPbF_2$ ($x = 0.10$, and 0.25 mol) glasses. *J. Eur. Ceram. Soc.*, 2007, **27**, 1801–1804.
4. Yukimitu, K., Oliveria, R. C., Araujo, E. B., Moraes, J. C. S. and Avanci, L. H., DSC studies on crystallization mechanisms of tellurite glasses. *Thermochim. Acta*, 2005, **426**, 157.
5. Mirgorodsky, A. P., Merle-Mejean, T., Camparnaud, J.-C., Thomas, P. and Frit, B., Dynamics of structure of TeO_2 polymorphs: model treatment of paratellurite and tellurite; Raman scattering evidence for new γ- and δ-phases. *J. Phys. Chem.*, 2000, **61**, 501–509.
6. Bueno, L. A., Messaddeq, Y., Dias Filho, F. A. and Ribeiro, S. J. L., Study of fluorine losses in oxyfluoride glasses. *J. Non-Cryst. Solids*, 2005, **351**, 3804–3808.
7. Villegas, M. A. and Fernandez Navaro, J. M., Physical and structural properties of glasses in the TeO_2–TiO_2–Nb_2O_5 system. *J. Eur. Ceram. Soc.*, 2007, **27**, 2715–2723.
8. Silva, M. A. P., Briois, V., Poulain, M., Messaddeq, Y. and Riberio, S. J. L., Lead–cadmium oxyfluoride glasses and glass–ceramics. *J. Phys. Chem. Solids*, 2002, **4**(3), 799–808.
9. Akagi, R., Handa, K., Ohtori, N., Hannon, A. C., Tatsumisago, M. and Umesaki, N., High-temperature structure of K_2O–TeO_2 glasses. *J. Non-Cryst. Solids*, 1999, 111–118, 256&257.
10. O'Donnell, M., *Tellurite and fluorotellurite glasses for active and passive fiber optic waveguides*. Ph.D. thesis. The University of Notthingham, UK, 2004.
11. Champarnaud-Mesjard, J. C., Blanchandin, S., Thomas, P. and Mirgorodsky, A., Crystal structure, Raman spectrum and lattice dynamics of a new metastable form of tellurium dioxide: γ-TeO_2. *J. Phys. Chem. Solids*, 2000, **61**, 1499–1507.
12. Blanchandin, S., Marchet, P., Thomas, P., Champarnaud-Mesjard, J. C. and Frit, B., New investigations within the TeO_2–WO_3 system: phase equilibrium diagram and glass crystallization. *J. Mater. Sci.*, 1999, **34**, 4285–4292.
13. Charton, P. and Armand, P., X-ray absorption and Raman characterizations of TeO_2–Ga_2O_3 glasses. *J. Non-Cryst. Solids*, 2004, **333**, 307–315.
14. Dewan, N., Sreenivas, K. and Gupta, V., Properties of crystalline γ-TeO2 thin film. *J. Cryst. Growth*, 2007, **305**, 237–241.
15. Öz, B., Kabalcı, I., Öveçoğlu, M. L. and Özen, G., Thermal properties and crystallization behavior of some TeO_2–K_2O glasses. *J. Eur. Ceram. Soc.*, 2007, **27**, 1823–1827.

16. Dietzel, A., Glasstruktur und Glaseigenschaften. *Glasstech Bre.*, 1948, **22**, 41–80.
17. Kabalcı, I., Özen, G., Öveçoğlu, M. L. and Sennaroğlu, A., Thermal study and linear optical properties of $(1-x)TeO_2$–$(x)PbF_2$ ($x = 0.10$,0.15 and 0.25 mol) glasses. *J. Alloy Compd.*, 2006, **419**, 294–298.
18. Cenk, S., Demirata, B. and Öveçoğlu, M. L., Özen, Thermal properties and optical transition probabilities of Tm^{3+} doped TeO_2–WO_3 glass. *Spectrochim. Acta A*, 2001, **57**, 2367–2372.
19. Özen, G., Demirata, B. and Öveçoğlu, M. L., Effect of composition on the thermal properties and spontaneous emission probabilities of Tm^{3+} doped TeO_2–LiC glass. *J. Mater. Res.*, 2001, **16**, 1381–1388.
20. Öveçoğlu, M. L., Özen, G. and Cenk, S., Microstructural characterization and crystallization behavior of $(1-x)TeO_2$–xWO_3 (x = 0.15, 0.25, 0.3 mol) glasses. *J. Eur. Ceram. Soc.*, 2006, **26**, 1149–1158.
21. Wang, G., Dai, S., Zhang, J., Wen, L., Yang, J. and Jiang, Z., Thermal, optical properties and structural investigation of TeO_2–$PbCl_2$ glassy system. *J. Phys. Chem. Solids*, 2005, 1–5.
22. Poulain, M. and Poulian, M., Multicomponent fluoride glasses. *J. Non-Cryst. Solids*, 1997, **213**, 40–43.
23. Nukui, A., Taniguchi, T. and Miyata, M., *J. Non-Cryst. Solids.*, 2001, **293**, 255.
24. Powder Diffraction Files: Card No. 42-1365, Database Edition, The International Centre for Diffraction Data (ICDD).
25. Powder Diffraction Files: Card No. 52-1005, Database Edition, The International Centre for Diffraction Data (ICDD).
26. Powder Diffraction Files: Card No. 49-1755, Database Edition, The International Centre for Diffraction Data (ICDD).